



**HAL**  
open science

## Heterodyne interferometric technique for displacement control at the nanometric scale

Suat Topsu, Luc Chassagne, Darine Haddad, Yasser Alayli, Patrick Juncar

► **To cite this version:**

Suat Topsu, Luc Chassagne, Darine Haddad, Yasser Alayli, Patrick Juncar. Heterodyne interferometric technique for displacement control at the nanometric scale. *Review of Scientific Instruments*, 2003, 74 (11), pp.4876-4880. 10.1063/1.1614858 . hal-00870597

**HAL Id: hal-00870597**

**<https://hal.science/hal-00870597>**

Submitted on 7 Oct 2013

**HAL** is a multi-disciplinary open access archive for the deposit and dissemination of scientific research documents, whether they are published or not. The documents may come from teaching and research institutions in France or abroad, or from public or private research centers.

L'archive ouverte pluridisciplinaire **HAL**, est destinée au dépôt et à la diffusion de documents scientifiques de niveau recherche, publiés ou non, émanant des établissements d'enseignement et de recherche français ou étrangers, des laboratoires publics ou privés.

# Heterodyne interferometric technique for displacement control at the nanometric scale

Suat Topcu,<sup>a)</sup> Luc Chassagne,<sup>b)</sup> Darine Haddad,<sup>c)</sup> and Yasser Alayli<sup>d)</sup>  
*Laboratoire LIRIS, Université de Versailles, 45 avenue des États-Unis, 78035 Versailles, France*

Patrick Juncar<sup>e)</sup>  
*BNM-INM/CNAM, 292 rue Saint-Martin, F 75141 Paris, France*

(Received 21 May 2003; accepted 11 August 2003)

We propose a method of displacement control that addresses the measurement requirements of the nanotechnology community and provide a traceability to the definition of the mètre at the nanometric scale. The method is based on the use of both a heterodyne Michelson's interferometer and a homemade high frequency electronic circuit. The system so established allows us to control the displacement of a translation stage with a known step of 4.945 nm. Intrinsic relative uncertainty on the step value is  $1.6 \times 10^{-9}$ . Controls of the period of repetition of these steps with a high-stability quartz oscillator permits to impose an uniform speed to the translation stage with the same accuracy. This property will be used for the watt balance project of the Bureau National de Métrologie of France. © 2003 American Institute of Physics. [DOI: 10.1063/1.1614858]

## I. INTRODUCTION

Tolerances in the manufacturing processes of high technologies and nanotechnologies become increasingly restrictive and already reach in some fields (such as microelectronics, micromechanics, genetic) the limit of industrial possibilities. Developments in these fields are conditioned by the capability both to make nanometric displacements and to measure and control dimensions with a nanometric uncertainty.<sup>1</sup> Ultraprecision translation stages know important overhangs since the beginning of the century. The performances of platforms given by the ratio travel over resolution increase by a factor 5–10 every ten years.<sup>2</sup> Presently, the best platforms can make subnanometric displacement over some millimeters. Needs consist now to control these displacements with an accuracy and a repeatability at the subnanometric range. Displacement measurements at this scale remain a competitiveness factor for these high-tech industries. Another problem is the traceability of displacement measurements at this scale. Due to their inherent accuracy and their traceability, Michelson's interferometer have become an attractive tool for the most demanding measuring applications. We present a method of displacement measurement and control based on the use of a heterodyne Michelson's interferometer. Our system allows to achieve nanometric displacement with a known step of 4.945 nm. The newness of our method is its intrinsic relative accuracy of  $1.6 \times 10^{-9}$  on the step value.

As the method is based on the use of a heterodyne interferometer, the principle of this apparatus is first presented. Then the description of our method is made. Experimental

results that prove the validity of our method are finally exposed.

## II. PRINCIPLE OF HETERODYNE OPTICAL INTERFEROMETRY

Heterodyne laser interferometry forms the basis of metrology in numerous high-precision displacement measurement applications. The principle of heterodyne interferometer is shown in Fig. 1. The laser source contains two orthogonal polarized beams with different angular frequencies ( $\omega_1, \omega_2$ ). Waves are assumed to propagate along the positive direction of the  $z$  axis of an  $s-p-z$  orthogonal, right-handed, Cartesian coordinate system (Fig. 1). Electromagnetic field components of the laser beam  $E_L(z, t)$  can be represented as

$$\begin{pmatrix} E_s(z, t) \\ E_p(z, t) \end{pmatrix} = \begin{pmatrix} |E_0| \exp[-i(\omega_2 t + \phi_{0s})] \\ |E_0| \exp[-i(\omega_1 t + \phi_{0p})] \end{pmatrix}, \quad (1)$$

where  $|E_0| = |E_s| = |E_p|$  represents the amplitude of the linear, simple harmonic oscillations of the electric-field components along the  $s$  and  $p$  axes,  $\phi_{0s}$  and  $\phi_{0p}$  represent the initial phases. A neutral density beamsplitter divides the laser beam in two parts. One part of the beam is directed to a combining polarizer and a detector resulting in an interference signal. This signal will be used as a *reference signal*. Only the alternating current is measured due to the use of a band-pass filter, eliminating both the dc component and optical frequencies. Using the Jones matrices,<sup>3–5</sup> the electric field component of the beam on photodiode 1 (PD1) is given by

$$\mathbf{E}_{\text{ref}} = B(\pi/4) \cdot \mathbf{N} \cdot \mathbf{E}_L, \quad (2)$$

where the Jones matrix for a polarizer with its optical axis oriented at  $45^\circ$  relatively of the  $s$  and  $p$  axes and for a 50/50 neutral density beamsplitter are, respectively,

<sup>a)</sup>Electronic mail: suat.topcu@ens-phys.uvsq.fr

<sup>b)</sup>Electronic mail: luc.chassagne@ens-phys.uvsq.fr

<sup>c)</sup>Electronic mail: darine.haddad@ens-phys.uvsq.fr

<sup>d)</sup>Electronic mail: alayli@physique.uvsq.fr

<sup>e)</sup>Electronic mail: juncar@cnam.fr

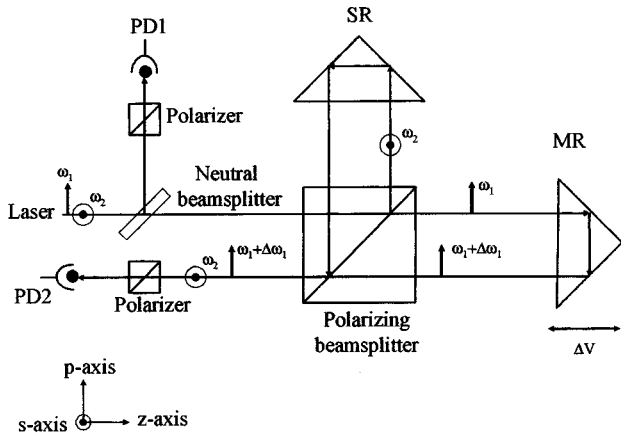


FIG. 1. Principle of the heterodyne interferometer: Two colinear and orthogonally polarized beams with different angular frequencies ( $\omega_1, \omega_2$ ) are sent on a polarizing beamsplitter. One of the beams is sent on a stationary retroreflector rather than the other which is sent on a movable retroreflector. Due to motion, this last beam is Doppler shifted. Both beams recombine at the back of the polarizing beamsplitter and interference occurs. The result is a phase shift of the measurement signal (PD2) compared to the reference signal (PD1). Displacement of the movable mirror could be deduced from this phase shift.

$$B(\pi/4) = \frac{1}{2} \begin{pmatrix} 1 & 1 \\ 1 & 1 \end{pmatrix}, \quad (3)$$

$$N = \frac{1}{2} \begin{pmatrix} 1 & 0 \\ 0 & 1 \end{pmatrix}. \quad (4)$$

After calculation, we obtain

$$E_{ref} = \frac{1}{4} E_0 \{ \exp[-i(\omega_2 t + \phi_{0s})] + \exp[-i(\omega_1 t + \phi_{0p})] \} \times \begin{pmatrix} 1 \\ 1 \end{pmatrix}. \quad (5)$$

The time-averaged intensity of the wave can be obtained by premultiplying their Jones vector  $\mathbf{E}$  by their Hermitian adjoint  $\mathbf{E}^\dagger$ , respectively. Then

$$I = cn \operatorname{Re}\{\mathbf{E} \cdot \mathbf{E}^\dagger\}, \quad (6)$$

where  $c$  is the speed of the light in vacuum and  $n$  the refractive index of air. Because a heterodyne interferometer only detects signals with frequency about  $(\omega_2 - \omega_1)$ , the dc terms can be discarded. Hence, the intensity of the reference signal is found to be

$$I_{ref} = \frac{1}{8} cn |E_0|^2 \cos[(\omega_2 - \omega_1)t + (\phi_{0s} - \phi_{0p})]. \quad (7)$$

The transmitted beam is once divided by a polarizing beamsplitter (PBS). It reflects one polarization of the incoming light to a stationary retroreflector (SR) (reference beam), and passes the other one to a movable retroreflector (MR) (measurement beam). The reference beam retraces its path after being reflected by the stationary retroreflector. The measurement beam is reflected by the movable retroreflector attached to an electromagnetic driver and moving at constant speed. As a result the measurement beam is Doppler shifted. The frequency shift is equal to twice the speed of the mirror divided by the wavelength of light. The measurement beam and the reference beam recombine at the back of the polarizing beamsplitter and interference occurs. The result is a phase shift of the measurement signal compared to the reference signal. In an ideal heterodyne interferometer, the  $p$  and  $s$  components of the electromagnetic field are perfectly separated by the PBS. Jones calculations lead to the electric field component of the beam on photodiode 2 (PD2):

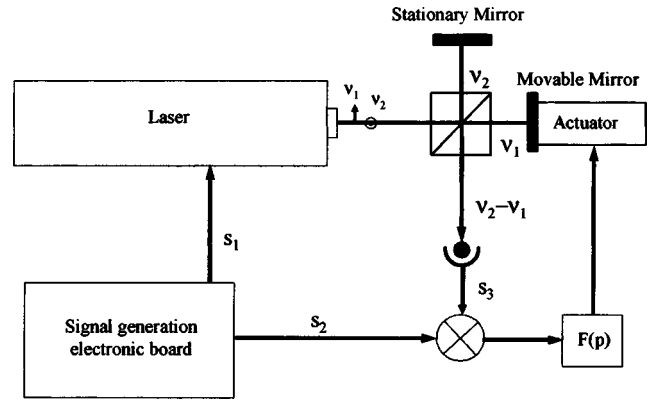


FIG. 2. Sketch of the phase-locked interferometric method for position and displacement control: An electronic board generates two synchronized signals  $s_1$  and  $s_2$  at the same frequency. Signal  $s_1$  is sent to the laser head rather than  $s_2$  which is sent on a mixer. Phases of both signals  $s_2$  and  $s_3$  (the electronic signal at the output of the interferometer) are compared. When a phase shift is made on  $s_1$  or  $s_2$ , signal error  $\epsilon$  becomes non-null and a motion of the mirror via the lock-in electronic is generated to compensate the phase shift by Doppler effect. If the phase shifts are quantified then it becomes possible to control the displacement of the translation stage step by step.

izing beamsplitter and interference occurs. The result is a phase shift of the measurement signal compared to the reference signal. In an ideal heterodyne interferometer, the  $p$  and  $s$  components of the electromagnetic field are perfectly separated by the PBS. Jones calculations lead to the electric field component of the beam on photodiode 2 (PD2):

$$E_{meas} = \frac{1}{4} E_0 \{ \exp[-i(\omega_2 t + \phi_{0s})] - \exp(-i\Delta\phi_1) \times \exp[-i(\omega_1 t + \phi_{0p})] \} \begin{pmatrix} 1 \\ 1 \end{pmatrix} \quad (8)$$

and so

$$I_{meas} = \frac{1}{8} cn |E_0|^2 \cos[(\omega_2 - \omega_1)t + (\phi_{0s} - \phi_{0p}) - \Delta\phi_1]. \quad (9)$$

The displacement of the movable retroreflector can be deduced from the phase difference between  $I_{ref}$  [Eq. (7)] and  $I_{meas}$  [Eq. (9)] using

$$\Delta\ell = \frac{\lambda_1 \Delta\phi_1}{4\pi}, \quad (10)$$

where  $\lambda_1$  represents the wavelength in air. Compared to homodyne Michelson's interferometers, in heterodyne interferometers, signal containing displacement information is translated to a frequency  $\Delta\omega = \omega_2 - \omega_1$  permitting hence a better signal to noise ratio.

### III. DESCRIPTION OF THE PHASE-LOCKED INTERFEROMETRIC METHOD

Neglecting refractive index of air fluctuations, a displacement of a movable mirror given by a one-pass Michelson's interferometer by an amount of  $\lambda/2$  corresponds to a phase shift equal to  $2\pi$ . The method we proposed here consists in reversing this property of Michelson's interferometers. Consider the sketch in Fig. 2. An electronic board generates two synchronized signals  $s_1$  and  $s_2$  at the same frequency  $\nu$ . Electronic circuit allows us to make phase

jumps of quantified value on either signals. Signals  $s_2$  and  $s_1$  are, respectively, sent to a mixer and to a laser head which transpose the signal from ultrasonic range to optical frequency range thanks to a Bragg cell. This allows to perform the two optical components of the heterodyne interferometer. The optical beam passes through the interferometer. The two components are recombined at the output of the interferometer, resulting on a signal  $s_3$  at the same frequency of  $s_1$  and  $s_2$ . Signal  $s_3$  contains position information then  $s_3$  is phase compared with  $s_2$  and a signal error is sent to a lock-in electronic that pilots an actuator supporting the movable mirror.

### A. Position and displacement control

Suppose the movable mirror moves away or closer to the polarizing beamsplitter. Doppler effect on the mirror results in a negative or positive phase shift compared to a phase of signals  $s_1$  or  $s_2$ . A non-null signal error  $\epsilon$  is then sent onto an integrator and the actuator acts upon the mirror to null this signal. We have realized a position looked loop system.

Suppose now that  $s_1$  or  $s_2$  undergo a phase shift by an amount of  $\Delta\phi$ . Here again,  $\epsilon$  becomes non-null and a motion of the mirror via the lock-in electronic is generated to compensate the phase shift by Doppler effect until phases of signals  $s_1$ ,  $s_2$ , and  $s_3$  become equal. Displacement value  $\Delta x$  of the mirror is directly related to the phase shift by the equation  $\Delta x = \lambda \Delta\phi / 4\pi$ . If the phase shift is quantified and equal to  $\Delta\phi = 2\pi/N$  where  $N$  is an integer, it becomes possible to control the displacement of the translation stage with a known step given by  $\Delta p = \lambda / 2N = c / 2N\nu$ . As the laser frequency  $\nu$  (or wavelength in vacuum) is one of the frequencies recommended by the Comité International des Poids et Mesures to realize the mètre, the traceability of the displacement measurements is assured at the nanometric scale.

### B. Speed control

If the period of repetition of these steps is stable (thanks to a high-stability quartz oscillator), we impose an uniform speed to the displacement of the movable mirror. The uncertainty on the value of the speed  $\theta$  could be as high as the uncertainty on step value. This uncertainty is given by

$$\frac{\sigma_{\bar{\theta}}}{\bar{\theta}} = \frac{2\sqrt{3}}{\eta^3} \frac{\sigma_{\bar{p}}}{\bar{p}}, \quad (11)$$

where  $\bar{\theta}$  is the mean value,  $\eta$  the step number,  $\sigma_{\bar{p}}$  the noise level on each step, and  $\bar{p}$  the mean value of a step.

## IV. EXPERIMENTAL SETUP AND RESULTS

### A. Description of the commercial heterodyne interferometer

A sketch of the commercial heterodyne system is shown in Fig. 3. A laser beam coming from a He-Ne frequency stabilized laser enters into an acousto-optic modulator (AOM) which generates two output beams. One of the beams (zero order) remains at the initial frequency  $\nu_1$  rather than the other (first order) is shifted in frequency by an amount of  $\Delta\nu$  equals to 20 MHz. These two waves are po-

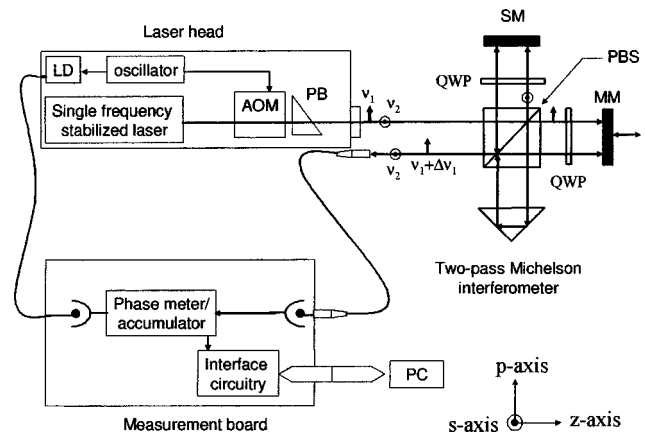


FIG. 3. Description of the commercial heterodyne interferometer: Interferometer used in our experiment is a ZMI2001 from Zygo. It is composed mainly by a laser source with two orthogonally polarized beams separated in frequency by 20 MHz. These two components are generated by an acousto-optic modulator (AOM) and a birefringent prism (BP). The Michelson's interferometer is a double-pass one. It is composed by a stationary mirror (SM), quarter waveplates (QWP), a polarizing beamsplitter (PBS), and a movable mirror (MM). The resolution of the system is 0.31 nm.

larized at  $45^\circ$  with respect to  $s$  and  $p$  axes. Both beams pass through a birefringent prism that divide each of them into two beams polarized along  $s$  and  $p$  axes. The main angle of the prism is designed to make colinear the  $s$ -polarized beam of the zero order wave with the  $p$ -polarized beam of the first order wave at the output of the prism.<sup>6</sup> At the output of the laser, the beam contains two monochromatic waves that are orthogonally polarized with slightly different wavelengths equal to  $\lambda_1 = 632.991\,528$  and  $\lambda_2 = 632.991\,501$  nm. The laser wavelength  $\lambda_1$  has been calibrated by beat frequency technic using a national reference with a relative uncertainty of  $1.6 \times 10^{-9}$ . Then, optical beam passes through a two-pass interferometer<sup>7</sup> before entering into an optical fiber pickup. There it passes through a polarizer that mixes the parallel and overlapping portions of the beam and a lens that couples the light into an optical fiber. The laser head outputs the reference signal at  $\Delta\nu = \nu_2 - \nu_1$  via also an optical fiber. The electronics measure the phase difference between both signals and process it to provide position and speed outputs. The system's resolution is limited by the system's noise and by the phase measurement method. The phase measurement has a dynamic error due to the variation between the time when the measurement signal transition occurred and when it is processed synchronously with the system clock. This time of  $\pm 1/2$  of the system clock's cycle results in a random position error, which appears as system noise proportional to the Doppler shift. The resolution of the system is 0.31 nm ( $\lambda/2048$ ). This corresponds to a phase resolution of  $360^\circ/512^\circ$ , or  $0.7^\circ$ , which is 97.7 ps at 20 MHz. This resolution is a factor of 2 better than that of any other commercially available system. Detailed informations concerning ZMI2001 interferometers could be found in Ref. 8.

### B. Experimental setup

Experimental setup is detailed in Fig. 4. An optical fiber connector on a front panel of the laser head, allows us to synchronize the laser frequency to an external reference os-

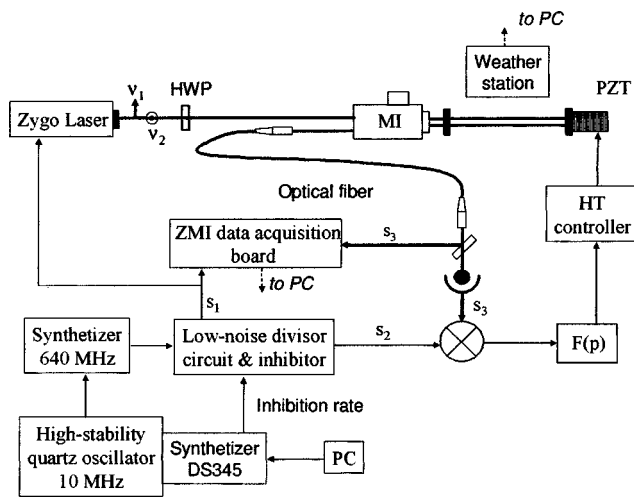


FIG. 4. Experimental setup: The laser head of the commercial interferometer is synchronized by an external reference signal coming from a homemade electronic circuit. At the output of the interferometer (MI), the beam is divided by a neutral density beamsplitter. One part of the beam is sent to the ZMI measurement board. The other part is sent to the PLL to lock in the mirror position via an integrator and a high voltage controller.

illator. Signals  $s_1$  and  $s_2$  are at frequency both equal to 20 MHz, generated from a homemade synthesizer with an ultrastable quartz oscillator ( $\sigma < 10^{-9}$  for  $1 \text{ s} < \tau < 1000 \text{ s}$ ). Initially, frequency of the synthesizer is equal to 640 MHz. A TTL signal at 10 MHz frequency issues from a digital synthesizer (DS345, Stanford) is used to synchronize the clock of our synthesizer. The DS345 is also used to generate a low frequency TTL signal which controls the inhibition of one period of the clock at 640 MHz using a command circuit composed by a logical PECL circuit. Each inhibition corresponds to a phase jump of  $2\pi$  on the signal at 640 MHz. This signal is then divided by a ratio of 32 using a low noise divisor circuit with digitally phase adjustment. Output of the divisor presents two signals both at 20 MHz frequency but with one presenting phase jumps. The DS345 is controlled by a PC board using an IEEE connection. The signal sent to the laser head is also sent to the ZMI2001 measurement board to calculate the displacement of the movable mirror using Eq. (10).

The beam coming from the laser is sent to a double-pass Michelson's interferometer (DPMI, Zygo). Movable mirror is mounted on a piezoelectric actuator (AE0203, Thorlabs). At the output of the interferometer, the beam is divided by a 50/50 neutral density beamsplitter. One part of the beam is sent to the ZMI2001 data acquisition system to measure the displacement value. The other part of the beam is sent to a mixer to be compared to  $s_2$  with quantified phase jumps. Error signal is sent to a high voltage controller to lock in the PZT actuator. Simultaneously, a weather station measures the room temperature, pressure, humidity content, and  $\text{CO}_2$  content. These values allow us to measure the fluctuations of the refractive index of air using Edlén equations.<sup>9</sup>

**V. RESULTS AND DISCUSSION**

Each time that a phase jump of  $2\pi/32$  occurred at the mixer, movable mirror do a step of  $\lambda/128$ . The wavelength of

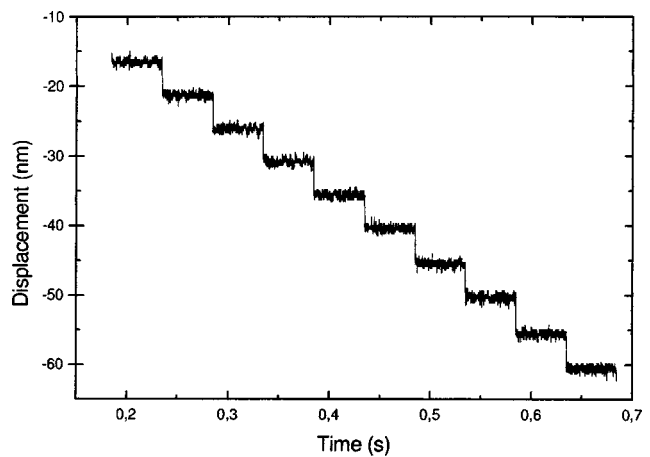


FIG. 5. Step by step displacement of the target mirror: We can see steps corresponding to phase jumps at the mixer level. Noise level on each step is equal to 0.22 nm (at  $1\sigma$ ).

the laser has been calibrated by Zygo and the nominal value is equal to  $\lambda_1 = 632.991\,528 \text{ nm}$ . Hence, we expect a step value of 4.945 nm. Relative uncertainty on the laser wavelength is  $1.6 \times 10^{-9}$ . So intrinsic uncertainty on the step value is  $8 \times 10^{-9} \text{ nm}$ . This value is the limit on accuracy that can be achieved with our method. Step by step displacement of the target mirror is depicted in Fig. 5. We can see steps corresponding to each phase jumps at the mixer. Noise level on each step is equal to 0.22 nm (at  $1\sigma$ ). Fluctuations of the room temperature, pressure, humidity content, and  $\text{CO}_2$  content are, respectively, 0.1 °C, 100 Pa, <1%, and 60 ppm. Using Edlén equations, refractive index of air variation is  $17 \times 10^{-8}$ . This corresponds to a negligible correction factor. This system of nanodisplacement and nanopositioning is dedicated to the watt balance project of the Bureau National de Métrologie (France). The aim of this project is to give a new definition to the mass unit.<sup>10</sup> One parameter to measure in this project is the speed of a moving coil. This speed will be equal to  $2 \text{ mm s}^{-1}$  and must be measured with an uncertainty of  $2 \text{ pm s}^{-1}$  (at  $1\sigma$ ). According to Eq. (11), the uncertainty on the speed of the movable mirror is inversely pro-

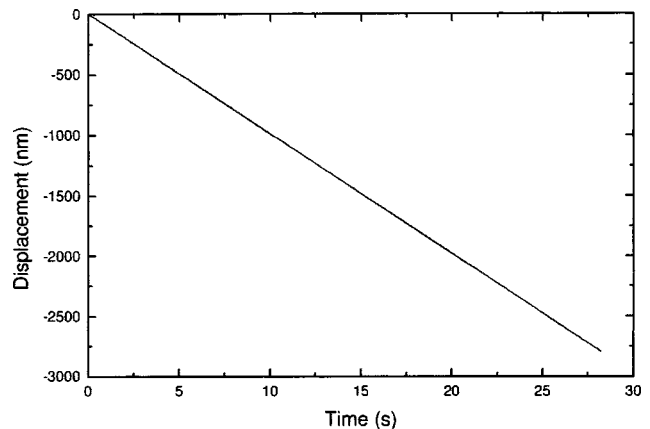


FIG. 6. Speed control of the target mirror composing the Michelson's interferometer: The slope of the curve is equal to the speed of the target mirror. This speed is imposed by the period of repetition of the phase jumps (i.e., 20 Hz). As each step is equal to 4.945 nm, the speed is hence equal to 98.904 (1)  $\text{nm s}^{-1}$ .

portional to the number of steps. The displacement range of the PZT actuator used in our experiment is limited to  $3\ \mu\text{m}$  for an applied voltage of 100 V. Note that our method does not have displacement range limit. The limit is only imposed by the translation stage used. This displacement is represented in Fig. 6. The slope of this curve is equal to the speed of the movable mirror. This speed  $\theta$  is imposed by the period of repetition of the phase jumps equal to 20 Hz. As each step is equal to 4.945 nm,  $\theta$  is equal to  $98.904(1)\ \text{nm s}^{-1}$ . Uncertainty on  $\theta$  is calculated with a step number  $\eta$  equal to 565 and a noise level on each step  $\sigma_{\bar{p}}$  equal to 0.22 nm at  $1\sigma$ . Relative uncertainty on the speed already reach  $1 \times 10^{-3}$ . To reach a relative uncertainty of  $10^{-9}$ , we need to make  $3 \times 10^5$  steps that is to say 1.5 mm of displacement. Displace-

ment range in watt balance project is planned to be 60 mm. Such uncertainty could be achieved with our method.

- <sup>1</sup>R. Leach, J. Haycocks, A. Lewis, S. Oldfield, and A. Yacoot, *Nanotechnology* **12**, 1 (2001).
- <sup>2</sup>H. Mizumoto, M. Yabuka, T. Shimizu, and Y. Kami, *Precis. Eng.* **17**, 57 (1995).
- <sup>3</sup>R. C. Jones, *J. Opt. Soc. Am.* **31**, 488 (1941).
- <sup>4</sup>R. C. Jones, *J. Opt. Soc. Am.* **31**, 500 (1941).
- <sup>5</sup>R. C. Jones, *J. Opt. Soc. Am.* **32**, 486 (1942).
- <sup>6</sup>Zygo, ZMI7702 Laser Head OMP-0402E.
- <sup>7</sup>Zygo, ZMI DPMI OMP-0223E.
- <sup>8</sup>F. C. Demarest, *Meas. Sci. Technol.* **9**, 1024 (1998).
- <sup>9</sup>K. P. Birch and M. J. Downs, *Metrologia* **30**, 155 (1993).
- <sup>10</sup>B. P. Kibble, J. H. Sanders, and A. H. Wapstra, *Atomic Masses and Fundamental Constants* (Plenum, New York, 1976), Vol. 5.